

DEFOCUS DEBLUR MICROSCOPY VIA FEATURE INTERACTIVE COARSE-TO-FINE NETWORK

Jiahe Wang, Boran Han

University of Wisconsin-Madison, Madison, WI 53715

ABSTRACT

The clarity of microscopic images is vital in biology research and diagnosis. When taking microscopy images at cell or molecule level, mechanical drift occurs and could be difficult and expensive to counter. Such a problem could be overcome by developing an end-to-end deep learning-based workflow capable of predicting in focused microscopic images from out-of-focused counterparts. In our model, we adopt a structure of multi-level U-net, each level connected head-to-tail with corresponding convolution layers from each other. In contrast to the conventional coarse-to-fine model, our model uses the knowledge distilled from the coarse network transferred to the finer network. We evaluate the performance of our model and found our method to be effective and has a better performance by comparing the results we got with existing models.

1. INTRODUCTION

The quality of images taken by microscopes is imperative to biology-related research as well as disease diagnoses, such as malaria and cancer detection. However, keeping the biology sample of the target in focus can be challenging due to the imperfect microscopy’s mechanical stability, i. e. mechanical drift [1]. Drift on the focal axis (z-direction) increasingly limits the resolution of advanced surface-coupled, single-molecule experiments. In the case of microscopes with a high-precision objective lens, samples taken at $1\ \mu\text{m}$ away from the focal plane can lead to image quality degradation. Such a high-precision objective lens can be essential for single-molecule tracking and molecule biology research. A conventional solution includes improving mechanical stability [2] or installing a real-time feedback system, such as focus lock [1, 3]. However, those out-of-focus (OOF) images can be wasted if mechanical drift can’t be corrected since such an inconvenient issue will lead to data re-acquisition.

An alternative solution to avoid data re-acquisition is to deblur the OOF image using image processing methods. Traditionally, deconvolution has been implemented to recover the in-focus (IF) images from OOF images [4]. This method usually requires to have point spread function (PSF) [4]. However in practice, finding the true PSF is impossible, and usually an approximation of it is used, theoretically calculated or based

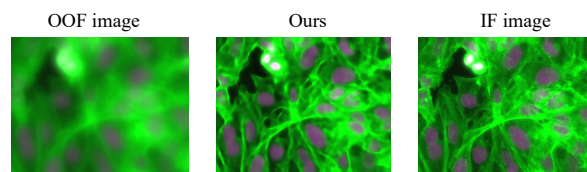


Fig. 1. Example OOF image (left), predicted IF images (middle) and ground truth IF images (right)

on some experimental estimation by using known probes. Recently, defocus deblurring using deep learning has become a popular topic thanks to convolution neural networks (CNN). Such methods are most commonly used to process blurred pictures taken by cameras [5, 6, 7]. In contrast to the conventional imaging system, i.e., camera, the microscopic image is also often required to be accurate. Despite the fact that limited methods have been introduced focuses on solving the deblurring problems for microscopy images [8, 9, 10, 11, 12], some of the methods are tested under synthetic defocus data [12, 8], while others either fail to provide an end-to-end method [9], or fail to test under objectives with high numerical aperture [12].

To overcome these limitations, we developed a end-to-end deep learning-based workflow to predict IF microscopic images from OOF counterparts, inspired by [13]. Our approach can lead to more efficient data acquisition. We adopt a multi-level U-net, with each level having interactions with other levels as it has been tested that would yield a better result. We demonstrated that our method has a superior performance compared with other competing methods. In summary, our contributions is as follows:

- We develop a new multi-level U-Net for defocus deblurring with the learned hidden features transferred from coarse level to fine level, facilitating learning efficiency
- We propose two interacting modes between subnetworks. Such two models yield similar performance.
- We demonstrate our method is superior to other state-of-the-art methods via testing on fluorescent microscopic images

2. METHOD

2.1. Prior knowledge

Problem defined. An OOF image (x) can be obtained from IF image (y) convoluted by the PSF at a given z :

$$x = y * PSF(z) + \epsilon \quad (1)$$

where $*$ is the convolution operator and ϵ is the noise. Since PSF is impossible to acquire, here we proposed a model $M : x \rightarrow y$ that can obtain y from x .

Coarse-to-fine network. As a pioneering work, DeepDeblur [13] directly learns the relation between blurry-sharp image pairs in an end-to-end manner by adopting a coarse-to-fine strategy. Each subnetwork consists of a sequence of convolutional layers that maintains the spatial resolution of input feature maps. Different scales of input images are fed into the sub-networks, and the resultant image from a coarser scale sub-network is concatenated with the input of a finer scale sub-network to enable coarse-to-fine information transfer. The reconstruction procedure of DeepDeblur [13] is formulated as follows:

$$\hat{y}_n = U_{\theta_n}^{(n)}(x_n; \hat{y}_{n+1} \uparrow) + x_n \quad (2)$$

where $U_{\theta_n}^{(n)}$ is the n -th subnetwork parameterized by θ_n . \hat{x}_n and \hat{y}_n are the blurred and predicted deblurred images at n -th scale. \uparrow are the upsampling operation. It is based on the assumption that the deblurred image can be obtained by the adding the fine details to the blurred images (Eq. 2). However such an assumption is not accurate in the microscopy system and can only yield an linear approximation of deconvolution, an operation inverse to get the OOF images (Eq. 1).

2.2. Defocus deblurring model

Inspired by the DeepDeblur [13], we proposed a novel nested deep blurring architecture. We exploit U-net [14] of each sub-network[15]. However, instead of learning the fine residual of the images and added to the blurred images, we transfer distilled information between hidden layers between the adjacent sub-networks. The output of n -th sub-network is obtained from blurred images and the output of $n+1$ -th sub-network. n -th sub-network ($U_{(\theta_n, \theta_{n-1})}^{(n)}$) is parameterized by θ_n^D and θ_{n-1}^D :

$$\hat{y}_n = U_{(\theta_n, \theta_{n-1})}^{(n)}(x_n; \hat{y}_{n+1} \uparrow) \quad (3)$$

In our model, $U^{(n)}$ is the encoder-decoder-based U-Net with symmetric skip connections that directly transfers the feature maps from the encoder to the decoder. In contrast to conventional U-net, the encoder $U^{(n)}$ of our model is also connected with the decoder of $U^{(n+1)}$, shown in Figure 2. Intuitively, our fine model can enable more efficient

learning via utilizing the knowledge distilled from coarse counterparts. Our architecture is inspired by knowledge distillation [16, 17]. In the knowledge distillation model, knowledge is distilled though the teacher's logit, which means the student is supervised by both groundtruth labels and teacher's logits. Despite that our defocus deblurring model does not requires semi-supervised learning, experiments show that knowledge distillation can facilitate the supervised learning. It is worth mentioning that In detail, the $U^{(n)}$ can be represented as $(E_0^{(n)}, E_1^{(n)}, \dots, E_i^{(n)}, \dots, E_I^{(n)})$ and $(D_0^{(n)}, D_1^{(n)}, \dots, D_i^{(n)}, \dots, D_I^{(n)})$, where $E_i^{(n)}$ and $D_i^{(n)}$ are i -th features maps in the encoder and decoder of $U^{(n)}$, respectively. As a result, $E_i^{(n)}$ can be obtained by the following equation:

$$E_i^{(n)} = F(E_i^{(n)}, D_{i-1}^{(n+1)}) \quad (4)$$

F is the feature learning function which takes the $E_i^{(n)}$ and $D_{i-1}^{(n+1)}$.

Likewise with other multi-scale deblurring networks, we use the multi-scale content loss function [13], where we found that L1 loss produces better results than MSE loss for our network. The content loss L is defined as follows:

$$L = \sum_{n=1}^N (\hat{y}_n - y_n)^2 \quad (5)$$

where N is the number of levels, or subnetworks.

2.3. Feature learning

We here propose two methods to learn the features: residual learning and feature concatenation. In residual learning mode, the learnt features from decoder layer in $n+1$ subnetwork ($D_{i-1}^{(n+1)}$) are added to encoder layer of n subnetwork ($E_i^{(n)}$):

$$E_i^{(n)} = E_i^{(n)} + D_{i-1}^{(n+1)} \quad (6)$$

Alternatively, $E_i^{(n)}$ can also be obtained by concatenating the $D_{i-1}^{(n+1)}$:

$$E_i^{(n)} = [E_i^{(n)} : D_{i-1}^{(n+1)}] \quad (7)$$

where $:$ is the concatenation operator. The above equation (Equation 7) depicts feature concatenation mode.

Relation to DeepDeblur [13]. Our model, describes in Eq. 3, depicts an end-to-end non-linear function between x and y via cascade coarse-to-fine hidden feature learning ($E_i^{(n)}$). However DeepDeblur [13] performs the coarse-to-fine learning in final output through residual learning (Δy).

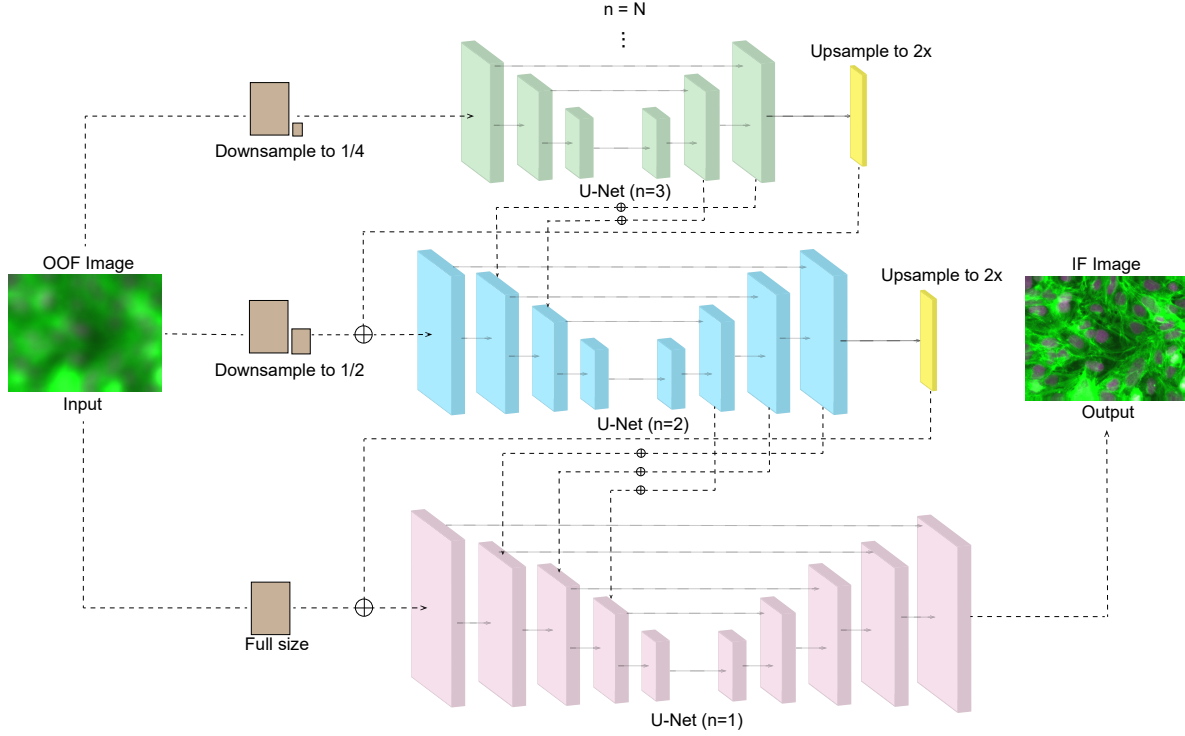


Fig. 2. The structure of our Model. OOF images will be downsampled and fed into corresponding multi-level U-Net. The learnt hidden features from the decoder of coarse sub-networks will be transferred to the encoder of the finer sub-networks, improving the training efficiency

3. EXPERIMENTS

3.1. Dataset

Our data sets come from the Broad Bioimage Benchmark Collection [18]. The data sets consist of 34 sets of microscopic images from human U2OS cells. The cells are stained with Hoechst 33342 markers and actin markers and imaged with an exposure of 15 and 1000 ms for Hoechst and phalloidin sequentially. All microscopic images are taken by objective with 20x magnification and two sites per well. For each site, the optimal focus was found via laser auto-focusing. The automated microscope was then programmed to collect a z-stack of 32 image sets with the step size of 2μ . As instructed by the dataset, we set $z = 17$ as our ground truth. Each z position consists of 768 pictures from different imaging areas. Each image is 696 x 520 pixels in 16-bit TIF format, LZW compression, two-color channels. In order to view the picture, one has to concatenate the two color channels of the respective picture. In our project, we assign the first 675 pictures as the training set, and the rest 93 images to be the testing set. We segment each image into four images with the size of 348 x 260 for ease of computation.

3.2. Experiment settings

We use Adam optimizer with learning rate 0.01, momentum 0.9, batch size 8. The network is usually trained for 80 epochs. All the following experiments were performed in a desktop with AMD Ryzen 7 5800X CPU and NVIDIA RTX 3080 GPU.

3.3. Ablation study

We evaluate our model using a various number of subnetworks ($N = 1 - 4$) and notice that performance improves as N increases. The result of 2-level U-net performs only slightly better than the original U-net model. However, when we added the third level and fourth level of U-net, the performance of the model increased remarkably. This result could be proven by the PSNR values shown in Table 1. We assess the two feature learning modes proposed in Section 2.3. Our results demonstrate that residual learning mode performs similar as the feature concatenation mode but has less trainable parameters.

Distance	34 μm	28 μm	22 μm	16 μm	10 μm	No. of trainable parameters
$N = 1$ (U-Net)	34.013	34.868	36.182	36.455	38.409	1,942,962
Residual learning mode						
$N = 2$	33.608	35.122	35.582	37.399	38.991	1,986,116
$N = 3$	34.641	35.619	36.418	37.474	39.831	2,543,478
$N = 4$	34.552	35.688	36.352	37.993	40.860	2,569,512
Feature concatenation mode						
$N = 2$	34.212	35.086	34.361	37.407	38.932	1,986,116
$N = 3$	33.928	35.402	36.298	37.914	39.725	2,543,478
$N = 4$	34.782	35.596	36.448	37.591	40.583	2,942,760

Table 1. PSNR values of our model with different number of levels (N), and different feature learning mode

Distance	34 μm	28 μm	22 μm	16 μm	10 μm
Input	32.048	32.421	32.915	33.732	35.404
Nah et. al. [13]	32.810	33.705	35.172	36.419	37.763
Liu et. al. [10]	31.011	32.872	34.030	35.098	37.199
Na et. al. [11]	31.409	31.908	32.513	34.804	37.253
Zhao et. al. [8]	34.125	35.153	36.412	37.995	40.420
Ours (residual learning mode)	34.552	35.688	36.352	37.993	40.860
Ours (feature concatenation mode)	34.782	35.596	36.448	37.591	40.583

Table 2. PSNR values of our model and other existing models. Best in bold.

Distance	34 μm	28 μm	22 μm	16 μm	10 μm
Input	0.736	0.757	0.786	0.830	0.895
Nah et. al. [13]	0.833	0.861	0.893	0.925	0.955
Liu et. al. [10]	0.717	0.770	0.844	0.905	0.946
Na et. al. [11]	0.728	0.728	0.807	0.890	0.940
Zhao et. al. [8]	0.826	0.864	0.895	0.928	0.962
Ours (residual learning mode)	0.848	0.880	0.899	0.929	0.967
Ours (feature concatenation mode)	0.845	0.870	0.898	0.929	0.958

Table 3. SSIM values of our model and other existing models. Best in bold.

3.4. Performance against other methods

To demonstrate our approach is able to accurately predict IF images, we compare our method with other existing methods, including methods from Nah et. al. [13], Liu et. al. [10], Na et. al. [11] and Zhao et. al. [8]. Among them, studies from Nah et. al. [13] has been demonstrated using camera images, such as GOPRO Dataset and Kohler Dataset[19], while the rest are specifically designed for optical or electron microscopic imaging domain. Liu et. al. [10] use residual connections for denoising and deblurring; Na et. al. [11] employ the multi-scale network consisting of several resnet; Zhao et. al. [8] adopt the residual densenet (RDN) [20], which is commonly used for super-resolution imaging. By measuring the SSIM and PSNR, it is shown that our proposed method can predict the IF images more accurately.

4. CONCLUSION

In this paper, we develop a new coarse-to-fine network with knowledge distillation for microscopic image deblurring. Our method shows superior results when tested with fluorescent imaging. The performance of our method in other imaging domains awaits future studies.

5. REFERENCES

- [1] Ashley R. Carter, Gavin M. King, Theresa A. Ulrich, Wayne Halsey, David Alchenberger, and Thomas T. Perkins, “Stabilization of an optical microscope to 0.1 nm in three dimensions,” *Appl. Opt.*, vol. 46, no. 3, pp. 421–427, Jan 2007.
- [2] Azeem Ahmad, Vishesh Dubey, Ankit Butola, Balpreet Singh Ahluwalia, and Dalip Singh Mehta, “Highly

- temporal stable, wavelength-independent, and scalable field-of-view common-path quantitative phase microscope,” *Journal of Biomedical Optics*, vol. 25, no. 11, pp. 116501, 2020.
- [3] P. P. Weafer, J. P. McGarry, M. H. van Es, J. I. Kilpatrick, W. Ronan, D. R. Nolan, and S. P. Jarvis, “Stability enhancement of an atomic force microscope for long-term force measurement including cantilever modification for whole cell deformation,” *Review of Scientific Instruments*, vol. 83, no. 9, pp. 093709, 2012.
 - [4] Jean-Baptiste Sibarita, *Deconvolution Microscopy*, pp. 201–243, Springer Berlin Heidelberg, Berlin, Heidelberg, 2005.
 - [5] Junyong Lee, Hyeonseok Son, Jaesung Rim, Sunghyun Cho, and Seungyong Lee, “Iterative filter adaptive network for single image defocus deblurring,” in *The IEEE Conference on Computer Vision and Pattern Recognition (CVPR)*, June 2021.
 - [6] Wenda Zhao, Cai Shang, and Huchuan Lu, “Self-generated defocus blur detection via dual adversarial discriminators,” .
 - [7] Junyong Lee, Sungkil Lee, Sunghyun Cho, and Seungyong Lee, “Deep defocus map estimation using domain adaptation,” in *The IEEE Conference on Computer Vision and Pattern Recognition (CVPR)*, June 2019.
 - [8] Huangxuan Zhao, Ziwen Ke, Ningbo Chen, Songjian Wang, Ke Li, Lidai Wang, Xiaojing Gong, Wei Zheng, Liang Song, Zhicheng Liu, Dong Liang, and Chengbo Liu, “A new deep learning method for image deblurring in optical microscopic systems,” *Journal of Biophotonics*, vol. 13, no. 3, pp. e201960147, 2020.
 - [9] Yichen Wu, Yair Rivenson, Hongda Wang, Yilin Luo, Eyal Ben-David, Laurent Bentolila, Christian Pritz, and Aydogan Ozcan, “Three-dimensional virtual refocusing of fluorescence microscopy images using deep learning,” *Nature Methods*, vol. 16, 12 2019.
 - [10] Jiahao Liu, Xiaoshuai Huang, Liangyi Chen, and Shan Tan, “Deep learning-enhanced fluorescence microscopy via degeneration decoupling,” *Opt. Express*, vol. 28, no. 10, pp. 14859–14873, May 2020.
 - [11] Juwon Na, Gyuwon Kim, Seong-Hoon Kang, Se-Jong Kim, and Seungchul Lee, “Deep learning-based discriminative refocusing of scanning electron microscopy images for materials science,” *Acta Materialia*, vol. 214, pp. 116987, 2021.
 - [12] Cheng Jiang, Jun Liao, Pei Dong, Zhaoxuan Ma, De Cai, Guoan Zheng, Yueping Liu, Hong Bu, and Jianhua Yao, “Blind deblurring for microscopic pathology images using deep learning networks,” *CoRR*, vol. abs/2011.11879, 2020.
 - [13] Seungjun Nah, Tae Hyun Kim, and Kyoung Mu Lee, “Deep multi-scale convolutional neural network for dynamic scene deblurring,” in *The IEEE Conference on Computer Vision and Pattern Recognition (CVPR)*, July 2017.
 - [14] Olaf Ronneberger, Philipp Fischer, and Thomas Brox, “U-net: Convolutional networks for biomedical image segmentation,” *CoRR*, vol. abs/1505.04597, 2015.
 - [15] Hongyun Gao, Xin Tao, Xiaoyong Shen, and Jiaya Jia, “Dynamic scene deblurring with parameter selective sharing and nested skip connections,” in *Proceedings of the IEEE/CVF Conference on Computer Vision and Pattern Recognition (CVPR)*, June 2019.
 - [16] Adriana Romero, Nicolas Ballas, Samira Ebrahimi Kahou, Antoine Chassang, Carlo Gatta, and Yoshua Bengio, “Fitnets: Hints for thin deep nets,” *CoRR*, vol. abs/1412.6550, 2015.
 - [17] Geoffrey E. Hinton, Oriol Vinyals, and Jeffrey Dean, “Distilling the knowledge in a neural network,” *ArXiv*, vol. abs/1503.02531, 2015.
 - [18] Vebjorn Ljosa, Katherine Sokolnicki, and Anne Carpenter, “Annotated high-throughput microscopy image sets for validation,” *Nature methods*, vol. 9, pp. 637, 06 2012.
 - [19] Rolf Köhler, Michael Hirsch, Betty Mohler, Bernhard Schölkopf, and Stefan Harmeling, “Recording and playback of camera shake: Benchmarking blind deconvolution with a real-world database,” in *Computer Vision – ECCV 2012*, Andrew Fitzgibbon, Svetlana Lazebnik, Pietro Perona, Yoichi Sato, and Cordelia Schmid, Eds., Berlin, Heidelberg, 2012, pp. 27–40, Springer Berlin Heidelberg.
 - [20] Yulun Zhang, Yapeng Tian, Yu Kong, Bineng Zhong, and Yun Fu, “Residual dense network for image super-resolution,” 2018.